CHAPTER 4

Review and Analysis of Modified Ripple Correlation Control MPPT for Single-stage Single-phase VSI Grid-connected Photovoltaic Systems

4.1 Introduction and outline

A grid-connected photovoltaic system (GCPVS) with single-stage single-phase voltage source inverter (VSI) is a direct power conversion from a photovoltaic (PV) array into the utility grid. It consists of a PV string, a decoupling capacitor, a half/full bridge inverter through the inductor and a controller unit, as shown in Figure 4.1. This topology is a buck type of string inverter where the suitable dc bus voltage is mostly required at the least highest peak value of the utility grid voltage. It is favored for among few kW power range due to its benefits of high efficiency and reliability, small size, uncomplicated control method, and low cost [2],[18],[45],[49]-[52]. With the controller unit, the maximum power point (MPP) of the PV string can be achieved continuously in every operating condition, and in the power control.

Unlike the two-stage, single-phase VSI GCPVS, there are two main groups, firstly, the first stage is performed by the high frequency dc-dc converter with the maximum power point tracking (MPPT) algorithm, and the high frequency dc-ac inverter is operating in the second stage. Secondly, the dc-dc converter of the first stage is similar to the previous group, but very different from its output waveform. This stage is controlled to generate an absolute sinusoidal current waveform. This waveform is then converted to the ac sinusoidal current by the unfolding dc-ac inverter in the second stage [53]-[60]. Consequently, both single- and two-stage VSI GCPVS require the MPPT algorithm in order to capture maximum power from the PV string and increase the efficiency of the PV system.

ลิขสิทธิ์มหาวิทยาลัยเชียงใหม่
Copyright© by Chiang Mai University
All rights reserved

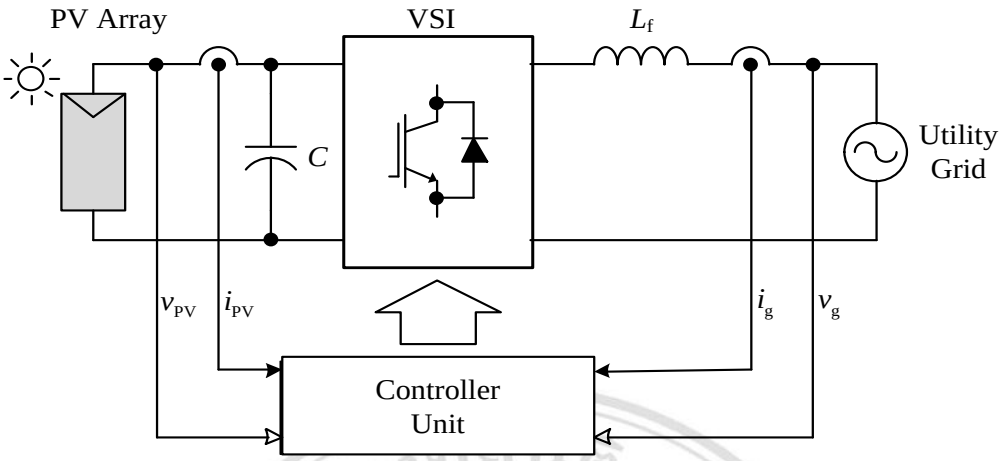

Figure 4.1 The power scheme of the single-stage single-phase VSI GCPVS.

Regarding the MPPT algorithms, the improved design of the perturb and observe (P&O) methods were presented in [31],[38],[61]-[63]. All of them provide a higher performance compared to the classical P&O method. A power measurement was proposed in [38] to identify exactly how much of the power change was produced from the change in irradiation called the optimized-P&O method. This method can track the MPP accurately. In [31], the direction of irradiation varying can be estimated correctly. Based on this method, the power losses caused by rapidly changing of irradiation can be reduced significantly. However, in order to accomplish the two solutions reported in [31] and [39], the controller still requires more time and the higher performance. In [62], a wide bandwidth dc voltage control loop of the P&O method was improved. However, this method is difficult to ensure the stability of the PV system at any operating condition. In [63], a proper design procedure for the sliding-mode controllers was compiled to ensure the stable MPPT requirements, but this method needed the low-pass (LP) filter and was much more complex than the classical P&O method. The hill climbing and the incremental conductance MPPT algorithm were reported in [2] and [8]. The performance of both MPPT methods depended on the sampling time and the step size of perturbation. On the other hand, the ripple correlation control (RCC) MPPT algorithms were proposed in [64]-[66]. Compared with the method in [38]-[39] and [61]-[62], the RCC-MPPT method does not need the step perturbation to achieve the MPP due to using the inherent gradient increment feature to approach the MPP, which can be easily implemented through an analog or digital circuit. The use of RCC-MPPT

ลิขสิทธิ์มหาวิทยาลัยเชียงใหม่
Copyright© by Chiang Mai University
All rights reserved

method for a dc-dc converter, to prove the high performance of this algorithm was reported in [64], [65]. An extreme seeking method for the RCC-MPPT method for a grid-connected inverter was proposed in [66]. Based on this method, the HP filter is still used to obtain the desired ripples. In [67], the modified extreme seeking control for a boost dc-dc converter was also reported. In [29], a combination between the RCC-MPPT method and the model reference adaptive control method was addressed to eliminate the overshoot produced by using the conventional MPPT algorithm. In addition, an RCC-MPPT method for the single-stage single-phase GCPVS was introduced in [66]. This method requires the first order HP and LP filters to generate the ripples of the PV power, the PV voltage, and also the desired average value of the ripple product. However, some of the drawbacks to these ripples and this average value depend on their time constants and the need to eliminate the ac component, included in the measured PV voltage, for a PI voltage controller. Most of these drawbacks affect to reduce the performance of tracking and in the efficiency of the PV system.

In order to remedy these drawbacks, the utilization of the moving average filter, sometimes called mean function, is used in many applications [69] and was firstly applied into the MPPT algorithm for the single-stage single-phase VSI GCPVS [69] and [70]. This is in order to modify the conventional RCC-MPPT method, where its better point is that it is able to simply and precisely extract the valid ac and dc components required in the MPPT method without the carefulness of the time constant designs in HP and LP filters and the increment of the ac component filter function in the PI dc voltage controller. In this chapter, the modified RCC-MPPT method for the single-stage single-phase VSI GCPVS is extended with more deep analysis and comprehensive study on the accounts of the mean function principle along with its modification in the proposed MPPT method, the selection of the suitable integral gain for an integrator in the proposed MPPT method, and the details of the cascade loop controllers for the single-stage single-phase VSI GCPVS. Other than that, it is challenged by the simulation results directly compared with the experimental results, which can confirm the feasibility of the proposed control scheme for the single-stage single-phase VSI GCPVS, and can also be compared with the existing and well-known RCC-MPPT and P&O MPPT methods.

ลิขสิทธิ์มหาวิทยาลัยเชียงใหม่
Copyright © by Chiang Mai University
All rights reserved

4.2 The modified RCC-MPPT scheme and implementations

4.2.1 Conventional RCC-MPPT Method

The zero of partial derivative of the PV power to the PV voltage $\partial p_{\mathrm{PV}} / \partial v_{\mathrm{PV}} = 0$ is the essential value used to verify the MPP of the PV system. Furthermore, the change in PV power ∂p_{PV} and the PV voltage ∂v_{PV} act as the ac components or the ripples of the PV power $\tilde{p}_{\mathrm{PV}}$ and the PV voltage $\tilde{v}_{\mathrm{PV}}$, respectively, which can be replaced as follow [66]:

$$\frac{\tilde{p}_{\mathrm{PV}}}{\tilde{v}_{\mathrm{PV}}} \cong \frac{\partial p_{\mathrm{PV}}}{\partial v_{\mathrm{PV}}} \cong 0. \tag{4.1}$$

In [31],[38],[61]-[63], the MPP of the PV systems are achieved by adapting the function of the derivative of power to voltage in terms of ripples in (4.1) to avoid the critical calculation of the instantaneous power and voltage ripples by averaging the product of these ripples with the PV voltage ripple $\tilde{v}_{\mathrm{PV}}$ as given by:

$$\frac{\partial p_{\mathrm{PV}}}{\partial v_{\mathrm{PV}}} \cong \frac{\dfrac{1}{T_{\mathrm{rip}}} \displaystyle\int_{t-T}^{t} \left(\tilde{p}_{\mathrm{PV}} \tilde{v}_{\mathrm{PV}} \right) dt}{\dfrac{1}{T_{\mathrm{rip}}} \displaystyle\int_{t-T}^{t} \tilde{v}_{\mathrm{PV}}^2 dt} \cong \frac{\overline{\tilde{p}_{\mathrm{PV}} \tilde{v}_{\mathrm{PV}}}}{\overline{\tilde{v}_{\mathrm{PV}} \tilde{v}_{\mathrm{PV}}}} \tag{4.2}$$

where T_{rip} is a cycle time of ripples. Based on (4.2), the sign of the derivative of power to voltage can be adapted directly along the average of the product $\overline{\tilde{p}_{\mathrm{PV}} \tilde{v}_{\mathrm{PV}}}$ due to the average of $\tilde{v}_{\mathrm{PV}}^2$ always being a positive value. Therefore, this sign value is adequate to track the MPP PV voltage as follows:

$$\mathrm{sign}\left(\frac{\partial p_{\mathrm{PV}}}{\partial v_{\mathrm{PV}}} \right) \cong \mathrm{sign}\left(\overline{\tilde{p}_{\mathrm{PV}} \tilde{v}_{\mathrm{PV}}} \right) \begin{cases} = +1 & if \quad v_{\mathrm{MPP}} > v_{\mathrm{PV}} \\ = 0 & if \quad v_{\mathrm{MPP}} = v_{\mathrm{PV}} \\ = -1 & if \quad v_{\mathrm{MPP}} < v_{\mathrm{PV}} \end{cases}. \tag{4.3}$$

ลิขสิทธิ์มหาวิทยาลัยเชียงใหม่
Copyright© by Chiang Mai University
All rights reserved

Three situations of the sign signal are $+1$, 0, and -1, and they are used to indicate an increase, standby, and decrease in the PV voltage v_{PV} for tracking the MPP PV voltage v_{MPP}, respectively. To achieve the sign as (4.3), the power and voltage ripples have to be obtained correctly as the basic theory of the ac components or ripples as calculated by:

$$\tilde{p}_{PV} = p_{PV} - \bar{p}_{PV} \text{ and } \tilde{v}_{PV} = v_{PV} - \bar{v}_{PV} \quad (4.4)$$

where $\bar{p}_{PV}$ and $\bar{v}_{PV}$ are the average PV power and PV voltage, respectively. Furthermore, a method to obtain the desired ripples exploited by the conventional RCC-MPPTs [29],[64]-[66] is to use the HP filter to avoid the dc component and the LP filters to average the product of ripples $\overline{\tilde{p}_{PV}\tilde{v}_{PV}}$. Although the use of the filters is not complex and easy to achieve the desired ripples or average with only one process, it still has some drawback with respect to the definitions of the suitable time constants for the HP and LP filters in order to produce the high level of accuracy of the sign signal, which is still required as a period of time to expand the time delay for indicating the MPP of the sign signal. As aforementioned, in order to improve the method to harvest the high performance MPP indicator with the desired sign signal, the modified RCC-MPPT method is then proposed using the mean function algorithm, which is discussed in Section 4.2.2

4.2.2 Proposed modified RCC-MPPT method

Using the proposed modified RCC-MPPT method, it is directly based on the operation of the sign signal, which is dependent on the average product between the ripples of PV power $\tilde{p}_{PV}$ and PV voltage $\tilde{v}_{PV}$, for tracking the MPP. With this method, the conventional method discussed in Section 4.2.1 is modified by applying the mean function principle, as further discussed in Section 4.2.3, instead of the HP and LP filters in order to extract the ac components, which are the ripples of PV power $\tilde{p}_{PV}$ and PV voltage $\tilde{v}_{PV}$, and the dc components, which is the average product $\overline{\tilde{p}_{PV}\tilde{v}_{PV}}$, respectively,

ลิขสิทธิ์มหาวิทยาลัยเชียงใหม่
Copyright© by Chiang Mai University
All rights reserved

as analyzed in Section 4.2.4. Subsequently, the relative selection of the suitable integral gain K_{dv} in the proposed MPPT algorithm is accordingly considered in Section 4.2.5. Additionally, the cascade loop control represented by the dc voltage controller and the grid-connected current controller is also addressed in Section 4.2.6.

4.2.3 Principle of mean function (MF)

The typical principle of the mean function in continuous-time domain [29], with the arbitrary input signal $x(t)$ can be defined as:

$$\overline{x}(t) = \frac{1}{T_w}\int_{t-T_w}^{t} x(\tau)\cdot d\tau \tag{4.5}$$

where T_w is the time window width to calculate the mean function of the input signal $x(\tau)$, and $(t-T_w) < \tau \le t$. In order to find out its behavior in frequency domain, taking the Laplace transforms into (4.5), the transfer function of the mean function can be expressed as

$$\mathrm{MF}_{\mathrm{DC}}(s) = \frac{\overline{X}(s)}{X(s)} = \frac{1-e^{-T_w s}}{T_w s} \tag{4.6}$$

Replacing $s = j\omega$ and $T_w = 0.01$ in (4.6), the characteristic of the mean function is represented in Figure 4.2 (a). In this figure, it is evident that the mean function can exactly block the ac component of the input signal $x(t)$ for all the integer multiples of the frequency $1/T_w$. That means it can well extract the dc component in the input signal $x(t)$, which has the fundamental frequency $f_w = 1/T_w$, with very good odd and/or even harmonic elimination.

Besides, the pure ac component of the arbitrary input signal $x(t)$ can be achieved by modifying the operation of the mean function as follows

ลิขสิทธิ์มหาวิทยาลัยเชียงใหม่
Copyright© by Chiang Mai University
All rights reserved

$$\tilde{x}(t) = x(t) - \bar{x}(t) = x(t) - \frac{1}{T_w}\int_{t-T_w}^{t} x(\tau)\cdot d\tau \tag{4.7}$$

Likewise, its frequency appearance can be checked by taking the Laplace transforms in (4.7) and therefore its transfer function is

$$\mathrm{MF}_{\mathrm{AC}}(s) = \frac{\tilde{X}(s)}{X(s)} = \frac{e^{-T_w s} + T_w s - 1}{T_w s} = 1 - \mathrm{MF}_{\mathrm{DC}}(s) \tag{4.8}$$

The bode plot of (4.8) is shown in Figure 4.2(b) with the ability of pure ac component extraction in the input signal $x(t)$. That means it can give the desired peak value without the shifting in the phase of the ac component for the case of the fundamental frequency of the input signal $x(t)$ being $f_w = 1/T_w$.

4.2.4 Modified RCC-MPPT

As shown in Figure 4.3, a key idea of the proposed modified RCC-MPPT method is the utilization of the mean function, as it is a very simpler theoretical principle and high precision of both dc and ac component extractions without complicated design of the relevant parameters in time constants compared to the others filters. In order to achieve the ripples of PV power $\tilde{p}_{\mathrm{PV}}$ and PV voltage $\tilde{v}_{\mathrm{PV}}$ from the measured instantaneous PV power p_{PV} and PV voltage v_{PV}, respectively, these ripples can be obtained by using the concept of (4.4), resulting in

$$\tilde{p}_{\mathrm{PV}} = p_{\mathrm{PV}} - 2f\int_0^{\frac{T}{2}} p_{\mathrm{PV}}dt \quad \text{and} \quad \tilde{v}_{\mathrm{PV}} = v_{\mathrm{PV}} - 2f\int_0^{\frac{T}{2}} v_{\mathrm{PV}}dt \tag{4.9}$$

ลิขสิทธิ์มหาวิทยาลัยเชียงใหม่
Copyright© by Chiang Mai University
All rights reserved

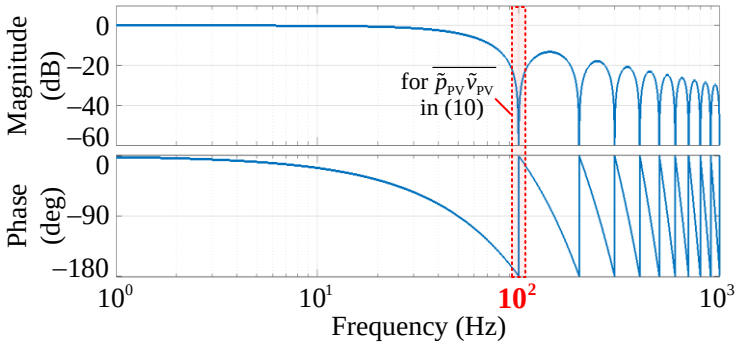

(a)

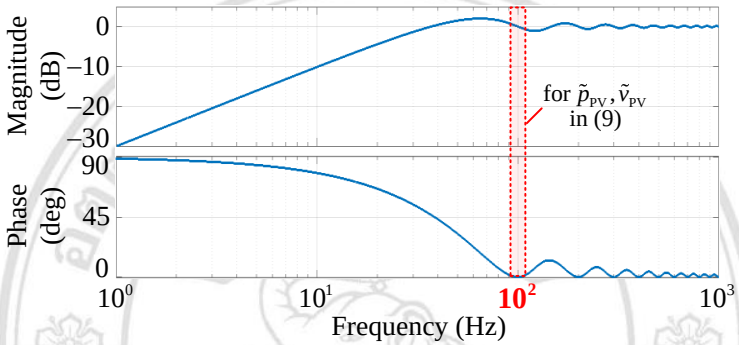

(b)

Figure 4.2 Bode plots of mean function principle for $f_w = 1/T_w = 100\,\text{Hz}$.
(a) DC component extraction. (b) AC component extraction.

In (4.9), due to the proposed MPPT method applied in the single-stage single-phase VSI GCPVS, $f = 50\,\text{Hz}$ in this case is the grid frequency and $T = 1/f$ is a time period of the grid. Thus, the frequencies of the ripples of both PV power $\tilde{p}_{PV}$ and PV voltage $\tilde{v}_{PV}$ are twice the grid frequency (100 Hz). Therefore, the time window widths for calculating the ripples of both PV power $\tilde{p}_{PV}$ and PV voltage $\tilde{v}_{PV}$ are designed to be $T_w = 1/2f = T/2 = 0.01\text{s}$, which leads to the pure ripples of the PV power $\tilde{p}_{PV}$ and PV voltage $\tilde{v}_{PV}$ with the desired peak values of the ripples and the constant 100-Hz frequency, as exemplified in the shadowed area of Figure 4.2 (a).

ลิขสิทธิ์มหาวิทยาลัยเชียงใหม่
Copyright© by Chiang Mai University
All rights reserved

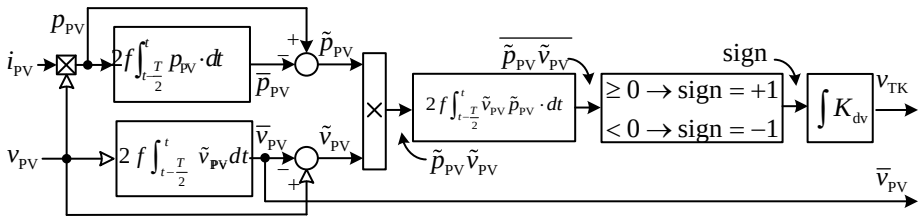

Figure 4.3 Block diagram of the proposed modified RCC-MPPT method.

After achieving the ripples of the PV power $\tilde{p}_{PV}$ and PV voltage $\tilde{v}_{PV}$ of (4.9), the product of the ripples $\tilde{p}_{PV}\tilde{v}_{PV}$ is then activated and its frequency still resembles the ripples of the PV power $\tilde{p}_{PV}$ and PV voltage $\tilde{v}_{PV}$. As a consequence, the average of that product $\overline{\tilde{p}_{PV}\tilde{v}_{PV}}$ can be subsequently generated to be forward to the processing of the sign signal computation by taking into consideration the concept of (4.5) as

$$\overline{\tilde{p}_{PV}\tilde{v}_{PV}} = 2f\int_{t-\frac{T}{2}}^{t} \tilde{p}_{PV}\cdot\tilde{v}_{PV}dt. \tag{4.10}$$

From (4.10), it is also done by using the same time window widths $T_w = T/2$ as for (4.9). That is why the dc component can be surely decomposed by blocking the 100-Hz product ripple $\tilde{p}_{PV}\tilde{v}_{PV}$ component, as illustrated in the shadow area of Figure 4.2 (a), as well as the other integer harmonic components in the product ripple $\tilde{p}_{PV}\tilde{v}_{PV}$. In addition, the average PV voltage $\overline{v}_{PV}$ is also obtained by the same algorithm of (4.10) in order to further use for the design of the dc voltage controller (see Section 4.2.6).

Next to the computation of the sign signal, it is carried out in the same way as (4.3) by using the comparing condition between the average product $\overline{\tilde{p}_{PV}\tilde{v}_{PV}}$ obtained from (4.10) and the reference zero in order to build the sign signal for tracking the MPP with a high precision and very convenient mathematical implementation based on account of the typical principle of the mean function.

ลิขสิทธิ์มหาวิทยาลัยเชียงใหม่
Copyright© by Chiang Mai University
All rights reserved

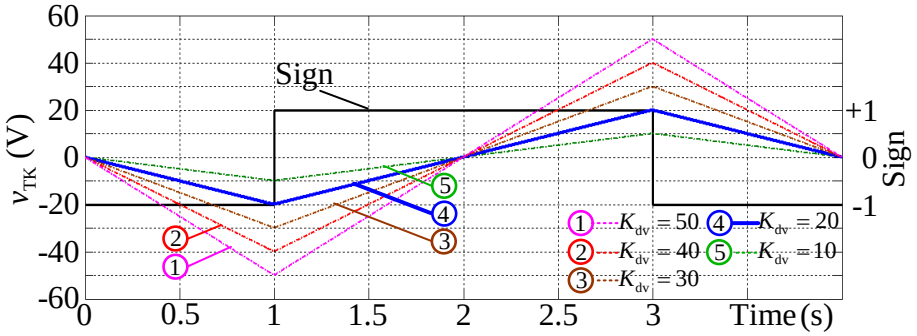

Figure 4.4 Criteria for selecting the integral gain K_{dv}.

However, the performance of the proposed MPPT method for the considerable system is also dependent on the defined value of the integral gain K_{dv}. For this reason, the selection principle of the suitable integral gain K_{dv} for the system is accordingly explained below.

4.2.5 Selection principle of integral gain

To generate a voltage waveform for MPP tracking follow the sign signal of $\overline{\tilde{p}_{PV}\tilde{v}_{PV}}$, an integrator, which produces a linear characteristic for the output with the speed depending on the slope offered by the integral gain K_{dv}, is used to transform the as given by

$$v_{TK} = \text{sign}\left(\overline{\tilde{p}_{PV}\tilde{v}_{PV}}\right)\cdot\left(\int K_{dv}dt\right) \tag{4.11}$$

where v_{TK} is the tracking voltage, which is a relative ramp output varying in accordance with the tracking of the input sign signal. K_{dv} is the integral gain of an integrator.

In order to reasonably select the suitable integral gain K_{dv} (see (4.11)) for achieving a good performance of the proposed MPPT algorithm for the single-stage single-phase VSI GCPVS, the simulated examples of the tracking voltages v_{TK} with five different integral gains K_{dv} of 50, 40, 30, 20, and 10 are illustrated in Figure 4.4, in a case study

ลิขสิทธิ์มหาวิทยาลัยเชียงใหม่
Copyright© by Chiang Mai University
All rights reserved

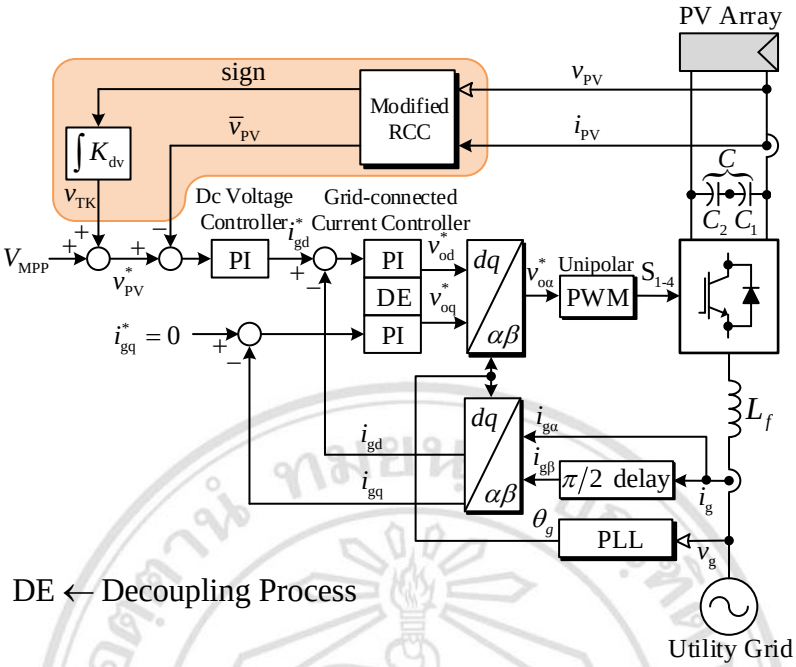

Figure 4.5 Power and control scheme of the proposed MPPT algorithm for single-stage single-phase VSI GCPVS.

of both upward (-1→0→+1) and downward (+1→0→-1) transitions of the sign signal. It is assumed that the sign signal attempts to track the MPP with the sampling time of 2 s for a visible description. In the figure, the sign signal is initially at -1, which leads to the continuous ramp-down of each tracking voltages v_{TK} (see lines ①, ②, ③, ④, and ⑤) from $t = 0$ s with their slopes corresponding to the integral gains K_{dv}. When the sign signal can meet the MPP at $t = 1$s, it is immediately changed to +1 and the tracking voltages v_{TK} are also changed to be ramp-up responses. It is evident that the tracking voltages v_{TK} with the high integral gain $K_{dv} = 50$ can reach to the MPP fastest than those of the other gains. However, it behaves as too big ripple, which is generally undesirable in the PI controllers. On the contrary, the tracking voltages v_{TK} may be too slow and not able to capture the MPP with the low integral gain $K_{dv} = 10$. Therefore, the use of the integral gain $K_{dv} = 20$ is selected and effective enough for the proposed MPPT method. That means it is fast enough for tracking the MPP with the agreeable

ลิขสิทธิ์มหาวิทยาลัยเชียงใหม่
Copyright© by Chiang Mai University
All rights reserved

compromise of the ripple magnitude of the tracking voltages v_{TK}, which is further transferred to part of the cascade loop controllers, as can be seen in Figure 4.5.

4.2.6 Cascaded loop controllers

In part of the dc voltage controller, the PV voltage reference v_{PV}^{*} is generated by summing the rated MPP voltage V_{MPP} and the tracking voltage v_{TK} given by (4.11) in order to control the PV voltage v_{PV} always operating on the MPP voltage V_{MPP}, and here it can be expressed as

$$v_{PV}^{*} = V_{MPP} + v_{TK} \tag{4.12}$$

where V_{MPP} is the initial value around the rated MPP voltage at the standard test condition (STC) of the PV array. To regulate the PV voltage v_{PV} following the MPP voltage of the PV array drawn by the reference PV voltage v_{PV}^{*}, the PI dc voltage controller is used for eliminating the steady-state error to achieve the MPP voltage, which is based on the Kirchhoff's current law at the connected point between the PV array, the capacitor and the inverter input terminals (see Figure 4.5) as given by

$$i_C = i_{PV} - i_{INV} = C\frac{dv_C}{dt} \tag{4.13}$$

where i_{INV} is the instantaneous input current of the inverter. Generally, the inverter and inductor filter (L_f) of the system are very small and have been omitted, the PV power p_{PV} is the summing of the instantaneous capacitor power p_C and the instantaneous grid power p_g, which is equal to the instantaneous input power of inverter p_{INV}, the reference grid power can be calculated as

ลิขสิทธิ์มหาวิทยาลัยเชียงใหม่
Copyright© by Chiang Mai University
All rights reserved

$$p_g^* = p_{INV}^* = v_{PV}(i_{PV} - C\frac{dv_C}{dt}) . \quad (4.14)$$

From (4.14), in order to avoid some ripples included in the reference grid power p_g^*, the instantaneous PV voltage v_{PV} can be replaced with the average PV voltage $\bar{v}_{PV}$, with the existing average PV voltage $\bar{v}_{PV}$, without extending the delay time.

In part of the grid-connected current controller, the main control objective of the proposed single-stage single-phase VSI GCPVS is to inject the active power into the grid with a unity power factor, which is based on the standard decoupling single-phase current control [51], [31]. From (4.3) and Figure 4.3, if the average PV voltage $\bar{v}_{PV}$ is higher than the reference PV voltage v_{PV}^*, the average PV voltage $\bar{v}_{PV}$ has to be reduced by increasing the grid current i_g, then v_{PV}^* is negative and $\bar{v}_{PV}$ is positive. The value of the reference PV voltage v_{PV}^* is compared with the average PV voltage $\bar{v}_{PV}$ to generate an error signal. This signal is fed into the PI voltage controller that determines the reference active power current component i_{gd}^* while the reference reactive power current component i_{gq}^* is

$$i_{gd}^* = \frac{2p_g^*}{V_{gd}} \text{ and } i_{gq}^* = \frac{2q_g^*}{V_{gd}} = 0 \quad (4.15)$$

where q_g^* is the reactive power, V_{gd}, V_{gq} are the $d-q$ axis grid voltage components, $V_{gd} = |\hat{v}_g|$ is the peak value of the grid voltage $\hat{v}_g$ whilst the grid voltage of q axis is set to zero, $V_{gq} = 0$. From (4.15), in order to generate the required reference inverter voltage, the PI current controllers with a decoupling process are used to regulate the reference inverter voltage components, v_{od}^* and v_{oq}^*, as calculated by

ลิขสิทธิ์มหาวิทยาลัยเชียงใหม่
Copyright© by Chiang Mai University
All rights reserved

$$\begin{bmatrix} v_{\mathrm{od}}^{*} \\ v_{\mathrm{oq}}^{*} \end{bmatrix} = L_f \frac{d}{dt}\begin{bmatrix} i_{\mathrm{gd}}^{*} \\ i_{\mathrm{gq}}^{*} \end{bmatrix} + \omega L_f \begin{bmatrix} -i_{\mathrm{gq}}^{*} \\ i_{\mathrm{gd}}^{*} \end{bmatrix} + \begin{bmatrix} V_{\mathrm{gd}} \\ 0 \end{bmatrix} \tag{4.16}$$

From the above equation, they are transformed to the $\alpha - \beta$ axis reference inverter voltage component $v_{o\alpha}^{*}$ by the position of the grid voltage (θ_{g}). A pulse width modulation (PWM) with unipolar technique is used to define the reference inverter voltage in the PWM block (see Figure 4.5).

4.3 Modeling studies of the modified RCC MPPT for single-stage single-phase VSI grid connected photovoltaic systems

A simulation model in MATLAB/Simulink is built to investigate the performance of the considerable system with the proposed MPPT method. It is operated under the comparison between the selective integral gain $K_{\mathrm{dv}} = 20$ and the other gains extending the discussion in Section 4.2.5, where the relevant parameters in Section 4.4 (see Table 4.1) were carried out, as shown in Figure. 4.6. In the first condition, the irradiance G_{i} steps down from 1000 $\mathrm{W/m^2}$ to 600 $\mathrm{W/m^2}$ (see Figure 4.6 (a)). As selected $K_{\mathrm{dv}} = 20$, the reference PV voltage v_{PV}^{*} in Figure 4.6 (b) and the reference active current i_{gd}^{*} in Figure 4.6 (c) are changed from the original MPP operation to the new MPP operation, where their speed MPP convergence is too much faster than that of the lower integral gain $K_{\mathrm{dv}} = 10$. However, it is almost the same as those of the higher integral gains, but behaving lower ripple, which is also better effectiveness to transfer and operate into the PI controllers in both dc voltage loop control and grid-connected current loop control (see the zoomed period in Figure 4.6 (c)). For the corresponding PV power p_{PV}, it can be seen in Figure 4.6 (d) that the MPP PV power can be achieved and has a good step change from around 952 W to 556 W according to the step change of the irradiance G_{i} for all of the considerable integral gains, due to the agreeable work of the cascade loop controllers. This can also examined by the corresponding *P-V* curve (Figure 4.6 (e)) from the MPP of period C to period D. After that, the next step-down change was from 600 $\mathrm{W/m^2}$ to 300 $\mathrm{W/m^2}$ and the returned-upward step changes also provided the same response, but only when operated at different MPP, as can be seen from the transition of

ลิขสิทธิ์มหาวิทยาลัยเชียงใหม่
Copyright© by Chiang Mai University
All rights reserved

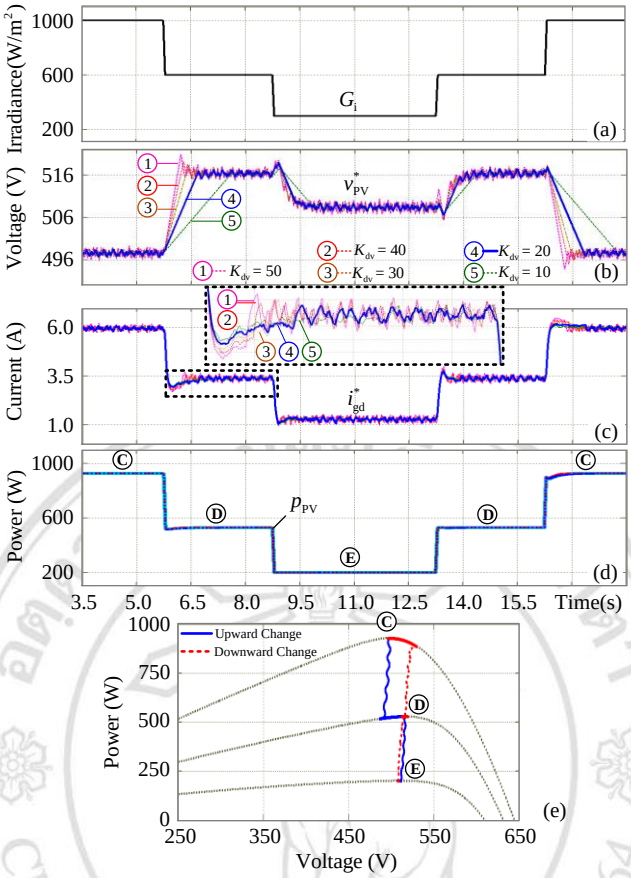

Figure 4.6 Dynamics of power and control performances.

the MPP in period D to period E and the upward changes from period E to period D and further to period C.

4.4 Experimental results

In this section, the proposed system presented by the single-stage single-phase VSI GCPVS and the modified RCC-MPPT method, as shown in Figure 4.5, has been verified by the simulation using the MATLAB/Simulink environment and the experimental implementation has been carried out on the laboratory prototype. It consists of two major parts. Part one is the controller using a dSPACE DS1104 controller via a CLP1104 Input/Output interface boards commanded by the programmable computer (PC) system, where the sampling time rates of the cascade loop control given by the dc voltage control and the grid-connected current control are set at 100 μs and 10 μs, respectively. The second part is the hardware included in the PV array source and the grid-connected VSI, which is controlled by the PWM signals with

ลิขสิทธิ์มหาวิทยาลัยเชียงใหม่
Copyright© by Chiang Mai University
All rights reserved

a deadtime of 4 μs. For a direct comparison, the parameters are set to be the same for both the simulation and experiment, as shown in Table 4.1. Significantly, the investigation is designed to regard the following points: i) to demonstrate the authentic precision of the proposed MPPT algorithm for the single-stage single-phase VSI GCPVS, ii) to demonstrate the dynamic performance of the proposed MPPT algorithm compared with the conventional methods applied in the single-stage single-phase VSI GCPVS for interfacing with the single-phase utility grid and to evaluate the efficiency of the proposed system.

Table 4.1 Main designed parameters of 3-Level VSI GCPVS

Parameters		Values
a-Si based PV module (LSU58, Kaneka):		
Maximum power in STC	(P_{MPP})	58 Wp
Open-circuit voltage in STC	(V_{oc})	85 V
MPP voltage and current in STC	(V_{MPP}, I_{MPP})	63 V, 0.92 A
PV Array:		
Rated power	(P_{rated})	928 W
Rated voltage and current	(V_{rated}, I_{rated})	504 V, 1.84 A
H-bridge VSI:		
Capacitors and inductor	(C_1, C_2)	2200 μF, 8 mH
Switching frequency	(f_{sw})	14 kHz
PI Controllers:		
Dc voltage controller	(K_{pv}, K_{iv})	0.08, 0.35
Grid-connected current controller	(K_{pc}, K_{ic})	15, 2000
Single-phase utility grid:		
Grid voltage and frequency	(V_g, f_1)	220 V, 50 Hz

ลิขสิทธิ์มหาวิทยาลัยเชียงใหม่
Copyright © by Chiang Mai University
All rights reserved

4.4.1 Precision of modified RCC-MPPT method

In addition to the reliability of the proposed modified RCC-MPPT method, Figure 4.7 shows the close-up operation during the leading edge of the sign signal. This is done by commanding the PV current i_{PV} from 0 A to 1.25 A. At the commencing (area A), the PV power p_{PV} is lower than the MPP. That means the MPP voltage is also lower than the PV voltage v_{PV}. Therefore, in this area, the average of ripple product $\overline{\tilde{p}_{PV}\tilde{v}_{PV}}$ is maintained below 0, leading to "-1" for the sign signal. Consequently, the PV power p_{PV} and the PV current i_{PV} are continuously increased, except that the PV voltage v_{PV} is reduced. When the PV power p_{PV} is identical to the MPP, the sign signal is precisely "0". It is noteworthy that the exact MPP occurs at the knee point of the PV power p_{PV} and it can also corroborate the methodical precision of the proposed MPPT algorithm. Next from the knee point, the PV voltage v_{PV} is lower than the MPP voltage and the sign signal is immediately changed to "+1", as shown in area B. The PV current i_{PV} and the PV voltage v_{PV} still increase and decrease, respectively. The PV power p_{PV} begins to reduce from the MPP, accordingly. Until the PV current i_{PV} is constrained to be a constant of around 1.25 A, all those variables are constant during the last 2 s period on the rightmost. On the other hand, the sign signal will be again changed from "+1" to "0" and "-1", respectively, when the PV voltage v_{PV} or the PV power p_{PV} are increased to the MPP. That means the proposed MPPT method will always track the MPP in order to keep its MPP constant. The good agreement between the simulation and experimental results can confirm the precision of the proposed MPPT method in both theoretical modeling and real plant systems, as shown in Figure 4.7 (a) and (b), respectively.

ลิขสิทธิ์มหาวิทยาลัยเชียงใหม่
Copyright© by Chiang Mai University
All rights reserved

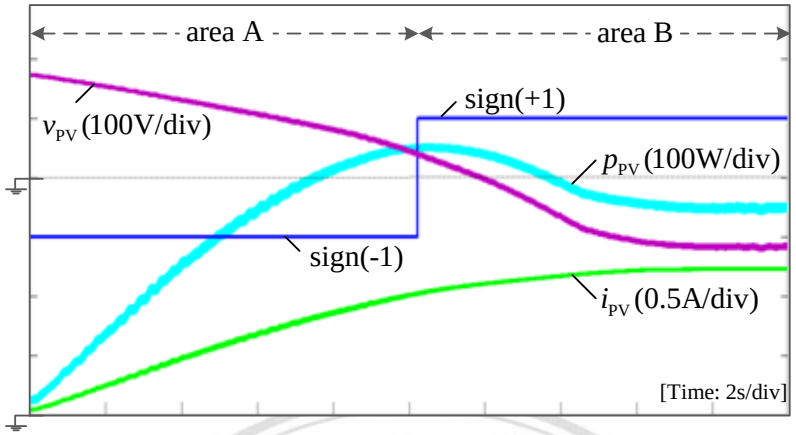

(a)

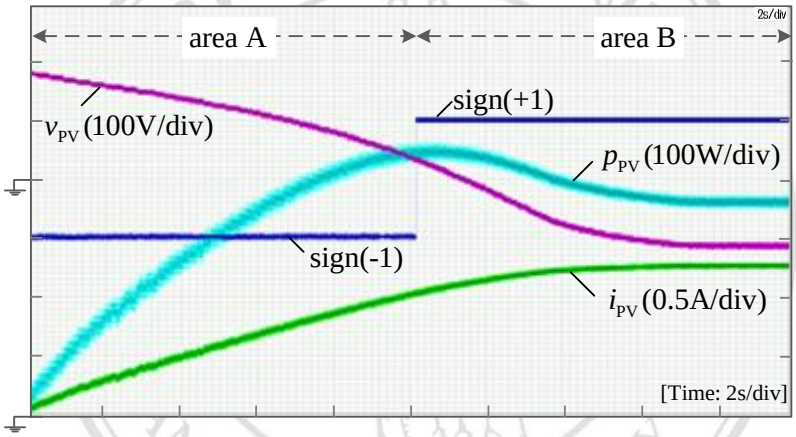

(b)

Figure 4.7 Verification in accuracy and precision of the proposed modified RCC-MPPT method by increasing the PV current i_{PV} from 0 A to 1.25A.

ลิขสิทธิ์มหาวิทยาลัยเชียงใหม่
Copyright© by Chiang Mai University
All rights reserved

4.4.2 Dynamic performance of modified RCC-MPPT method

The step response of the system based on the proposed modified RCC-MPPT method is shown in Figure 4.8. At period D, the PV power p_{PV} is initially at the MPP around 36% of the rated power with a single string of the PV array, and then, it is changed to 72% of the rated power at period C by connecting the other remaining string to the PV array. Although the slight deviation of the PV voltage v_{PV} is drawn at the transient period, as observed in Figure 4.8 (a) (see second trace), the system with the proposed MPPT method can immediately track the MPP. This can also be inspected

with the slight error position of the MPP voltage in the corresponding *P-V* curve at period D before changing into the MPP of period C. The grid-connected active current i_{gd} accordingly gives a critical damped stepped-up response, while the reactive component can be commanded to keep constant at zero, as shown in the third trace. Therefore, on the next trace it is pointed out that the unity power factor of the voltage and current for the grid side can be achieved in both steady-state and dynamic operations. Subsequently, these aforementioned responses also conduct in the same way as the challenge of the stepped-down PV power from period C to period D. The experimental results are demonstrated in good agreement with corresponding behavior, as shown in Figure 4.8 (b). Sequentially, the instantaneous grid voltages v_g and currents i_g in steady state of period D and period C are shown in Figure 4.9 (a) and (b) with a good unity power factor expression and THD_i qualities below 5% by 2.74% and 1.29%, respectively.

ลิขสิทธิ์มหาวิทยาลัยเชียงใหม่
Copyright© by Chiang Mai University
All rights reserved

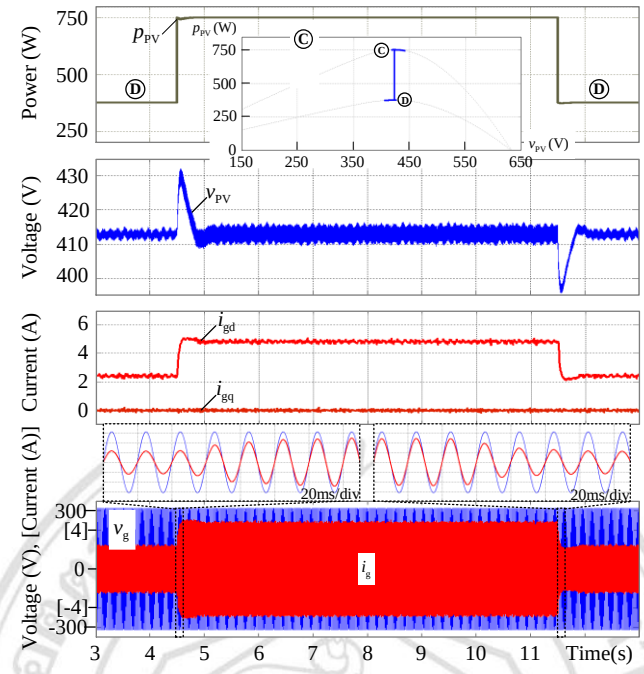

(a)

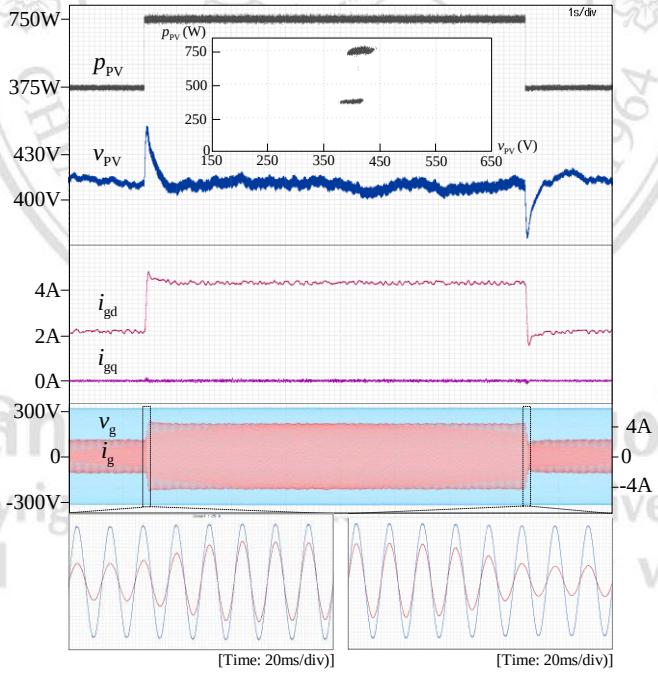

(b)

Figure 4.8 Dynamic response of the system using the proposed modified RCC-MPPT method for the step change of PV power.

ลิขสิทธิ์มหาวิทยาลัยเชียงใหม่
Copyright© by Chiang Mai University
All rights reserved

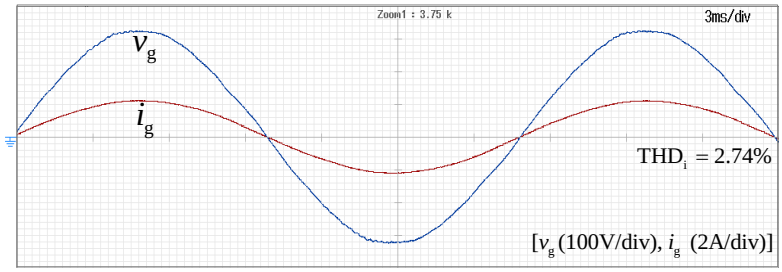

(a)

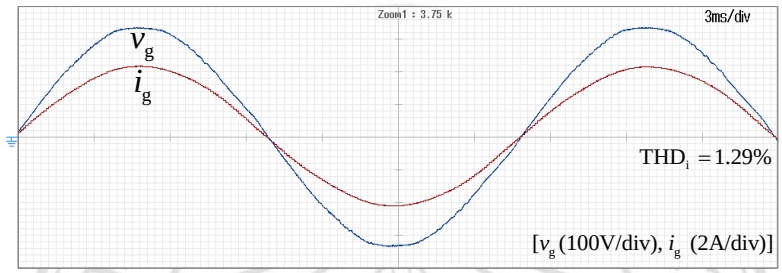

(b)

Figure 4.9 Steady-state experimental waveforms of the grid voltage v_g and current i_g.

To demonstrate the sudden variation in the irradiance, the dynamic linear shading results of the simulation and experiment are shown in Figure 4.10 (a) and (b), respectively. The PV power p_{PV} along with the PV current i_{PV} are found to have a linear change by the time $\Delta t = 0.3$ s. This leads to the same change in the grid current i_g. Moreover, the *P-V* curves are also shown with the corresponding operating points and it can ensure the validity of the MPPT approach.

Figure 4.11 shows the comprehensive performance of the proposed modified RCC-MPPT method (see Figure 4.11 (a)) since the starting to steady-state operation included the shading condition compared with the conventional RCC-MPPT method (see Figure 4.11 (b)) and the P&O MPPT method (see Figure 4.11 (c)). The realistic solar irradiances in the simulation are set to $920\,\mathrm{W/m^2}$, $882\,\mathrm{W/m^2}$, and $910\,\mathrm{W/m^2}$ for testing the proposed MPPT method, the RCC-MPPT method, and the P&O MPPT method, respectively, due to a direct comparison with the experimental results of each method

ลิขสิทธิ์มหาวิทยาลัยเชียงใหม่
Copyright© by Chiang Mai University
All rights reserved

with the uncontrollable irradiance in a real plant, as shown in Figure 4.12 (a), (b), and (c), respectively; however, these values are not much different.

With the proposed MPPT method in Figure 4.11 (a), the system is initially operated without the MPPT algorithm and hereby the utility grid is fed by 0 W along with the absences of PV and grid currents, except that the PV voltage reaches around 618 V, as it is the open-circuit voltage of the PV array. This operating period can be investigated at period A in the corresponding *P-V* curve. When the proposed MPPT algorithm is started during period B, the proposed MPPT algorithm attempts to track the MPP from this period to period C with the increments of the PV power and current, but the PV voltage is decreased relative to this. Hereby, the instantaneous injection of the grid current via the H-bridge VSI is then conducted. Until the PV power reaches to the MPP at 736 W in period C, the PV current and voltage is around 1.61 A and 480 V, as it is theoretically analyzed to be around 79% of the open-circuit voltage. As expected, it can supply a 700-W power into the interfacing utility grid. Continuing from this test, the 50% shading condition is also examined by disconnecting a PV string, as shown from period C to period D, where the response is similar to the stepped-down response from period C to period D of the prior case study discussed in Figure 4.8. In comparison between the proposed MPPT method and the two results of the conventional methods, the responses of the system in these three MPPT methods are the same. That is to say the performance of the proposed modified RCC-MPPT method is able to track the MPP, no matter if it's the starting or dynamic changing or steady-state even if it is any possible shading conditions, where its performance is in a good way equivalent to those of the existing and well-known RCC-MPPT and P&O MPPT methods.

ลิขสิทธิ์มหาวิทยาลัยเชียงใหม่
Copyright© by Chiang Mai University
All rights reserved

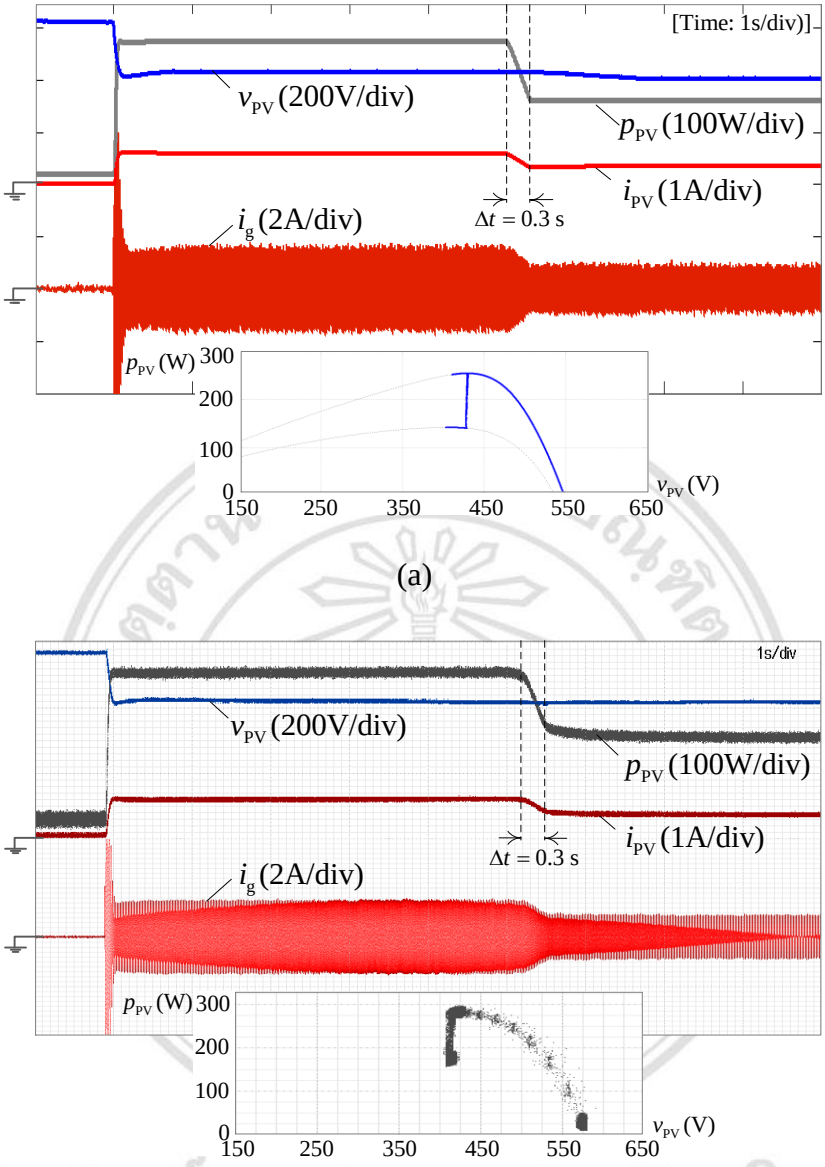

Figure 4.10 Dynamic response of the system using the proposed modified RCC-MPPT method for the linear shading of PV power.

ลิขสิทธิ์มหาวิทยาลัยเชียงใหม่
Copyright© by Chiang Mai University
All rights reserved

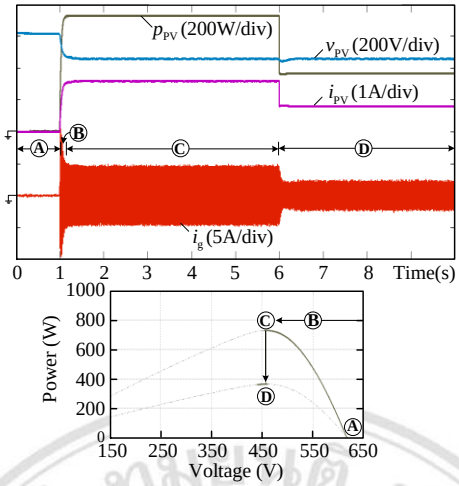

(a) Proposed modified RCC-MPPT method.

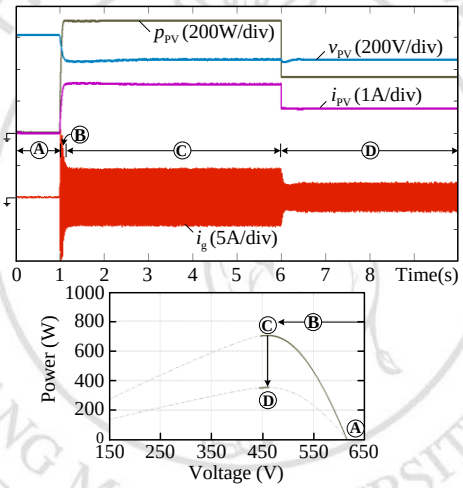

(b) Conventional RCC-MPPT method.

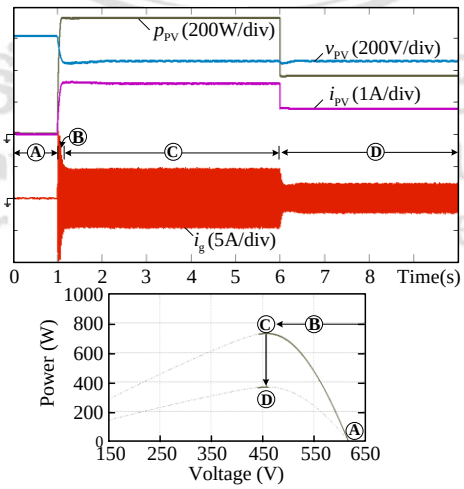

(c) Conventional P&O MPPT method.

Figure 4.11 Simulation results of the system response since starting operation.

ลิขสิทธิ์มหาวิทยาลัยเชียงใหม่
Copyright© by Chiang Mai University
All rights reserved

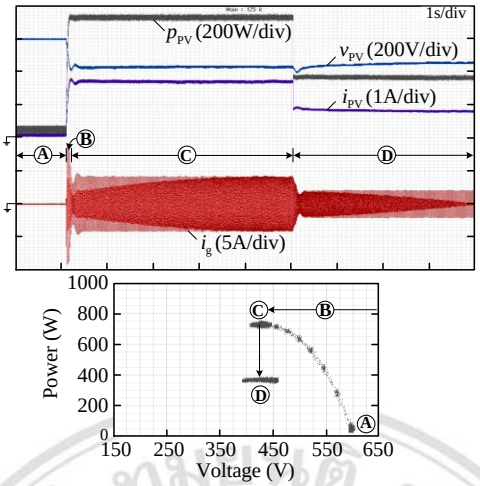

(a) Proposed modified RCC-MPPT method.

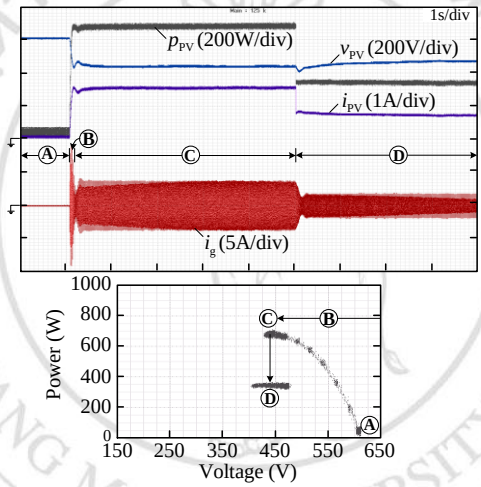

(b) Conventional RCC-MPPT method.

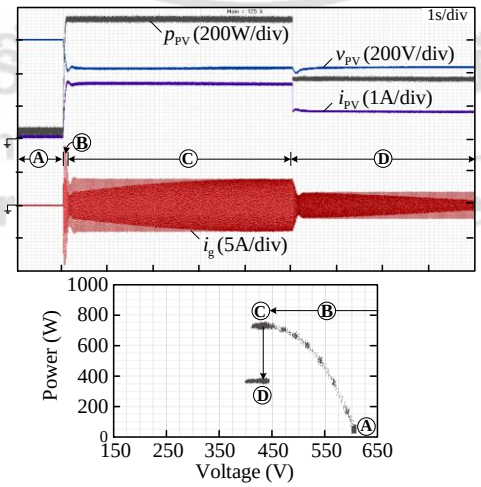

(c) Conventional P&O MPPT method.

Figure 4.12 Experimental results of the system response since starting operation.

ลิขสิทธิ์มหาวิทยาลัยเชียงใหม่
Copyright© by Chiang Mai University
All rights reserved

To evaluate the efficiency of the single-stage single-phase VSI GCPVS with the proposed modified RCC-MPPT method, the data loggers of the system efficiency are captured at various output grid powers under the variable realistic solar irradiation for four hours, as shown in Figure 4.13. The MPP voltages obtained by the proposed MPPT algorithm throughout the power from 0 W to 810 W are around 423 V to 582.9 V, which are successfully around 79% of the 618-V open-circuit voltage according to the theoretical MPP in the *P-V* characteristic. Moreover, the recognizable efficiency of more than 90% can be achieved since 200-W grid power on and the best measured value reach up to around 95% , where the corresponding experimental results can be seen in Figure 4.8 (b) and Figure 4.12 (a) at 700-W grid power with 423-V PV voltage. It is pointed out that the single-stage single-phase VSI GCPVS can get a gain high efficiency without the dc voltage control as with the two-stage system, as well as the dc-dc boost converter, through the robustness and flexibility of the controller and hardware, based on the proposed MPPT algorithm. On the other hand, the system efficiency falls in the light load condition (below 200-W grid power) owing to the increasing influences of the power losses caused by the active and passive components in the system.

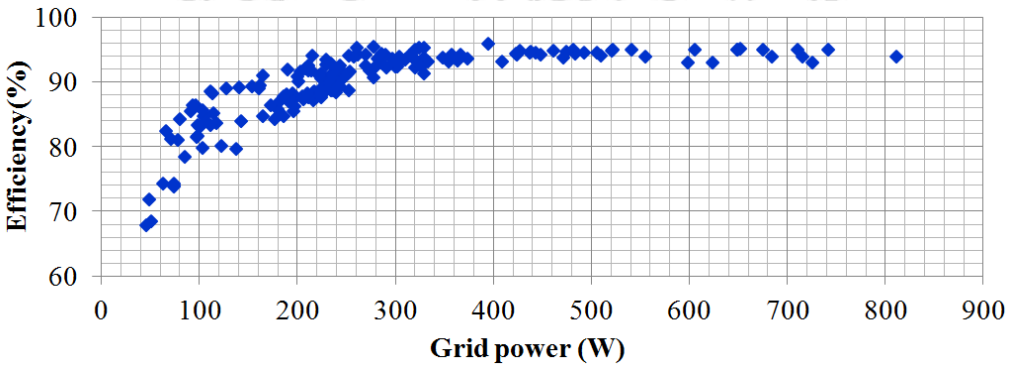

All rights reserved

Figure 4.13. Measured data loggers of system efficiency.

4.5 Conclusion

In this chapter, a modified RCC-MPPT algorithm using the simple mean function arithmetic was proposed and validated for the single-stage single-phase VSI grid-connected PV system. The mathematical model of the proposed RCC-MPPT method was discussed and was analyzed in detail by using Matlab/Simulink programs. This algorithm does not need the filters for generating the PV power and PV voltage ripples, and the average value of the ripple product. In addition, an ac component filter is not required in the part of a PI voltage controller. A high accuracy and precision MPPT was achieved during steady-state and dynamic shading operating conditions. The simulation and experimental results confirm the performance of the proposed control algorithm on a 1 kWp single-stage single-phase VSI grid-connected PV system. Next chapter will have discussed with the modified RCC-MPPT algorithm for the single-phase cascaded H-bridge multilevel inverter grid-connected PV system.

ลิขสิทธิ์มหาวิทยาลัยเชียงใหม่
Copyright© by Chiang Mai University
All rights reserved